Study on etch characteristics of magnetic tunnel junction materials using rf-biased H$_2$/NH$_3$ reactive ion beam

Ye Eun Kim, iD **Doo San Kim, Yun Jong Jang, et al.**

View Online   Export Citation   CrossMark

Study on etch characteristics of magnetic tunnel junction materials using rf-biased H₂/NH₃ reactive ion beam

View Online   Export Citation   CrossMark

Ye Eun Kim,[1] Doo San Kim,[1] Yun Jong Jang,[1] Hong Seong Gil,[1] Ho Seop Jeon,[1] Jong Woo Hong,[1] In Ho Kim,[2] Cheol Kim,[2] Jeong-Heon Park,[2] and Geun Young Yeom[1,3,a]

AFFILIATIONS

[1]School of Advanced Materials Science and Engineering, Sungkyunkwan University, Suwon 16419, Republic of Korea
[2]Advanced Process Development Team, Samsung Electronics, Hwaseong, Republic of Korea
[3]SKKU Advanced Institute of Nano Technology (SAINT), Sungkyunkwan University, Suwon 16419, Republic of Korea

Note: This paper is part of the Special Topic Collection Celebrating the Achievements and Life of Joe Greene.
[a]Electronic mail: gyyeom@skku.edu

ABSTRACT

In order to etch CoFeB and MgO constituting the magnetic tunnel junction (MTJ) layer of magnetic random access memory, rf-biased reactive ion beam etching (RIBE) with a H₂:NH₃ gas mixture was introduced and the etching characteristics were investigated. The H₂:NH₃ gas mixture of 8:1 was used for rf-biased RIBE because the etch selectivity is increased with H₂ percentage in the H₂:NH₃ gas mixture while the etch rates of MTJ materials are the highest between 2:1 and 1:1 ratio of H₂:NH₃ due to the synergy effect of H₂ and NH₃ in the etching of MTJ materials. When a high rf power was applied to the substrate (high rf-biasing) during RIBE, even though etch rates of MTJ materials were increased, the etch selectivities of MTJ materials over hard mask materials were decreased possibly due to the high physical sputtering effect. However, when small rf-biasing was added to the substrate during RIBE, improved etch characteristics such as higher etch selectivity of MTJ over the top electrode (TE) material, improved etch anisotropy of the MTJ pattern masked with TE, and a thinner sidewall residue on the MTJ pattern could be observed. The improvement in etch characteristics by the addition of small rf-biasing during RIBE is believed to be related to the increased chemical etching effect through H₂/NH₃ gas dissociation and the increased H/NH ratio in the plasma generated just above the substrate without increasing the physical sputtering effect. Specifically, for the substrate located on the insulating substrate holder, the charging of the substrate could be removed without using an electron emitting neutralizer by supplying electrons from the plasma generated by rf-biasing during RIBE.

I. INTRODUCTION

Spin transfer torque magnetic random access memory (STT-MRAM), which uses the changes in the magnetic direction for electrical characteristics, is known to be one of the most promising candidates for next-generation memory devices due to nonvolatility and high level of integrity of the device.[1–4] The STT-MRAM requires a magnetic tunnel junction (MTJ) consisted of two ferromagnetic layers such as CoFeB and an insulating layer such as MgO between the two magnetic layers. One of the two ferromagnetic layers is a free layer that can change the magnetization direction, and the other is a fixed layer with a fixed magnetization direction. If electron spin directions of the free layer and the fixed layer are the same, the current flows through the device; otherwise, the current does not flow due to the tunneling magnetoresistance effect in the MTJ cell.[5,6]

In general, for etching of MTJ materials, reactive ion etching (RIE) using halogen compounds such as Cl₂/Ar, CF₄/Ar, etc., cannot be used due to the low volatility of etch products and chemical damage to the magnetic material caused by halogen reactive ions and radicals.[7,8] Currently, a physical etching technique using an Ar⁺ ion beam, that is, ion beam etching (IBE), is mainly used for the fabrication of STT-MRAM devices.[9,10] However, physical

etching by the Ar$^+$ ion beam causes problems such as low etch rate, low etch selectivity over mask materials, and redeposition of a non-volatile metal on the sidewall of the etched MTJ cell. To remove the materials redeposited on the sidewall and to obtain anisotropic etch profiles, a tilted Ar$^+$ ion beam is used while the substrate is rotating. However, these techniques cannot be applied for the next-generation nanometer scale and high-density STT-MRAM due to the limited tilting angle of the Ar$^+$ ion beam caused by the decrease in the critical dimension of the pattern width and the high aspect ratio of the hard mask layer. The metallic sidewall residue remaining on the MgO surface will cause electrical short of the MTJ stack between the fixed layer and the free layer.[11–14]

Research studies have reported etching studies using reactive gases such as CH_3OH/Ar, CO/NH_3, etc., that could potentially form volatile metal carbonyl compounds to increase the etch rate and etch selectivity of magnetic materials and to obtain anisotropic etch profiles.[15–20] But these gas mixtures could decrease the magnetic properties of the MRAM after etching possibly due to oxygen decomposed from the plasmas.[10,21] Reactive ion beam etching (RIBE) using H_2/NH_3 has been also studied to reduce the surface damage caused by oxygen and to improve the etch profile.[22–24] In general, RIBE can precisely control the energy of ions compared to RIE and can obtain more anisotropic etch profiles; however, without overetching of MTJ materials to the substrate, it still seems to be difficult to remove the sidewall residue formed on the MTJ surface sufficiently. In addition, to operate the Ar$^+$ ion beam or RIBE, an electron emitting neutralizer is required to remove the charging of the substrate by positive ions especially when the substrate is located on the insulating substrate holder, and during the ion beam operation, the neutralizer can contaminate the substrate or can be easily damaged.[25]

When rf plasmas are generated on the substrate during RIBE, the etch characteristics such as etch selectivity, sidewall residue, etc., could be improved by increasing the chemical etching effect, and substrate charging could be removed by electrons in the plasma generated on the substrate surface. Therefore, in this study, radio frequency (rf) power was applied to the substrate (rf-biasing) during etching of MTJ materials using RIBE with H_2/NH_3 gas mixtures, and the effects of rf-biasing on etch characteristics such as etch rates, etch selectivity, etch profiles of magnetic materials, etc., and on the possibility of removing the charging on the substrate that replaces the neutralizer were investigated. In addition, the degree of sidewall residue remaining after MTJ etching was compared between RIBE and rf-biased RIBE.

II. EXPERIMENTAL

Figure 1(a) shows a schematic diagram of the rf-biased reactive ion beam etching system used in the experiment. For the reactive ion beam, an inductively coupled plasma (ICP) source installed with a grid assembly was located at the top of the processing chamber. The ICP source was operated with 13.56 MHz rf power, and the reactive ions were extracted and accelerated from the ICP ion beam source to the processing chamber located below the source. The grid assembly was consisted of three grids made of molybdenum. A positive voltage was applied to the first grid to control the energy of the ions, a negative voltage to the second grid
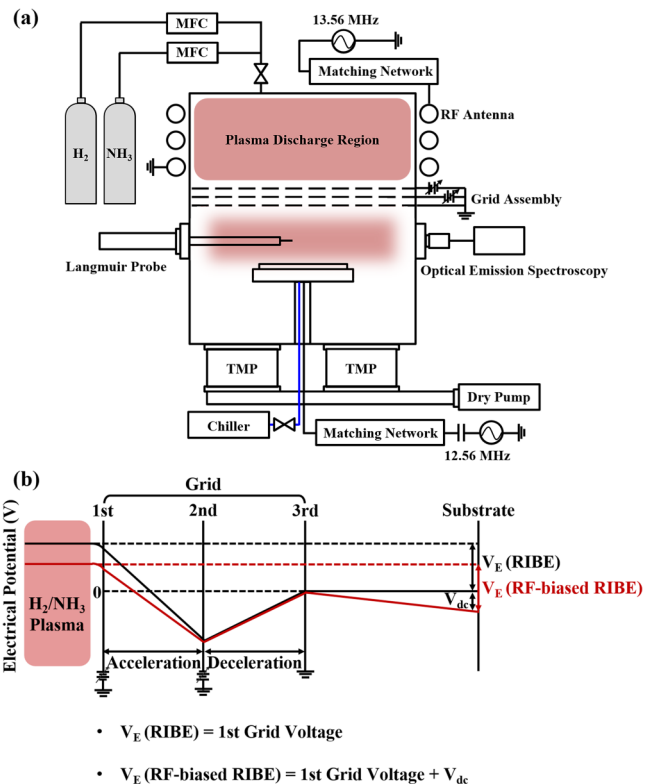

FIG. 1. (a) Schematic diagram of the rf-biased reactive ion beam etching (rf-biased RIBE) system composed of a three-grid type ion source and substrate rf biasing. (b) Electrical potentials V_E between the ion source and the substrate during RIBE and rf-biased RIBE. The net electrical potential is first grid voltage + V_{dc} (for RIBE, $V_{dc} = 0$).

to control the flux of the extracted ions, and the ground potential to the third grid. The substrate was grounded or negatively biased by applying 12.56 MHz rf power to the substrate for the operation as RIBE and rf-biased RIBE, respectively. The substrate was located on the metallic substrate holder or on the ceramic plate covered substrate holder. During the rf-biased RIBE, an additional plasma was formed above the substrate holder.

MRAM materials such as CoFeB and MgO and mask materials such as the hardmask (HM) and the top electrode (TE) were sputter deposited on Si wafers for the measurement of etch characteristics. In addition, an MTJ structure of CoFeB/MgO/CoFeB deposited on bottom electrode (BE)/Si wafers was dot-patterned with a mask of HM/TE for the observation of MTJ etch profiles. For etching, gas mixtures composed of H_2/NH_3 were used while keeping 1 mTorr of pressure at the process chamber and the substrate temperature was kept at 20 °C using a chiller. The ICP power was kept at 300 W and the first grid voltage was varied from −250 to −150 V while keeping the second grid voltage at −200 V. The H_2/NH_3 gas mixture was also varied from 10:1 to 0:1. In the case of rf-biasing, a negative potential, −V_{dc}, is developed on the substrate in addition to the potential difference between the first grid voltage

(first grid V) and the ground (0 V) from the ion beam source; therefore, the ion energy bombarding the substrate is increased to first grid $V + V_{dc}$ for rf-biased RIBE while the ion energy to the substrate for RIBE is related to only first grid voltage as shown in Fig. 1(b).

The cross sections of the thin films were observed by field emission scanning electron microscopy (FE-SEM, Hitachi, S-4700) to measure the etch depth, etch rates, and etch profiles of the etched MTJ materials and hard mask materials. After MTJ pattern etching, high resolution transmission electron microscopy (JEOL, JEM ARM 200F) was used to observe redeposition on the sidewall. The Image J program was used to measure the RMS edge roughness of the etched MTJ dot pattern. After RIBE and rf-biased RIBE, the surface chemistry of etched CoFeB and TE was observed by x-ray photoelectron spectroscopy (XPS, ESCA 2000, VG Microtech Inc.) using an Al K_α twin-anode source. In order to analyze

plasmas generated above the substrate during rf-biasing, optical emission spectroscopy (OES, Verity, SD1024F) and a single Langmuir probe (APL-150, Impedans) were used to measure the species in the plasmas and the electron density, respectively.

III. RESULTS AND DISCUSSION

The etch rates of MTJ and mask materials and their etch selectivities measured for different gas mixture ratios of H_2/NH_3 for RIBE are shown in Figs. 2(a) and 2(b), respectively, and those for different dc bias voltages ($-V_{dc}$) of rf-biased RIBE added to a fixed RIBE condition are shown in Figs. 2(c) and 2(d). As MTJ materials, CoFeB and MgO were used, and as mask materials, TE and HM were used. As the substrate holder, an Al substrate holder maintained at RT by a chiller and connected to the ground potential for the removal of substrate charging was used. 1 mTorr of operating
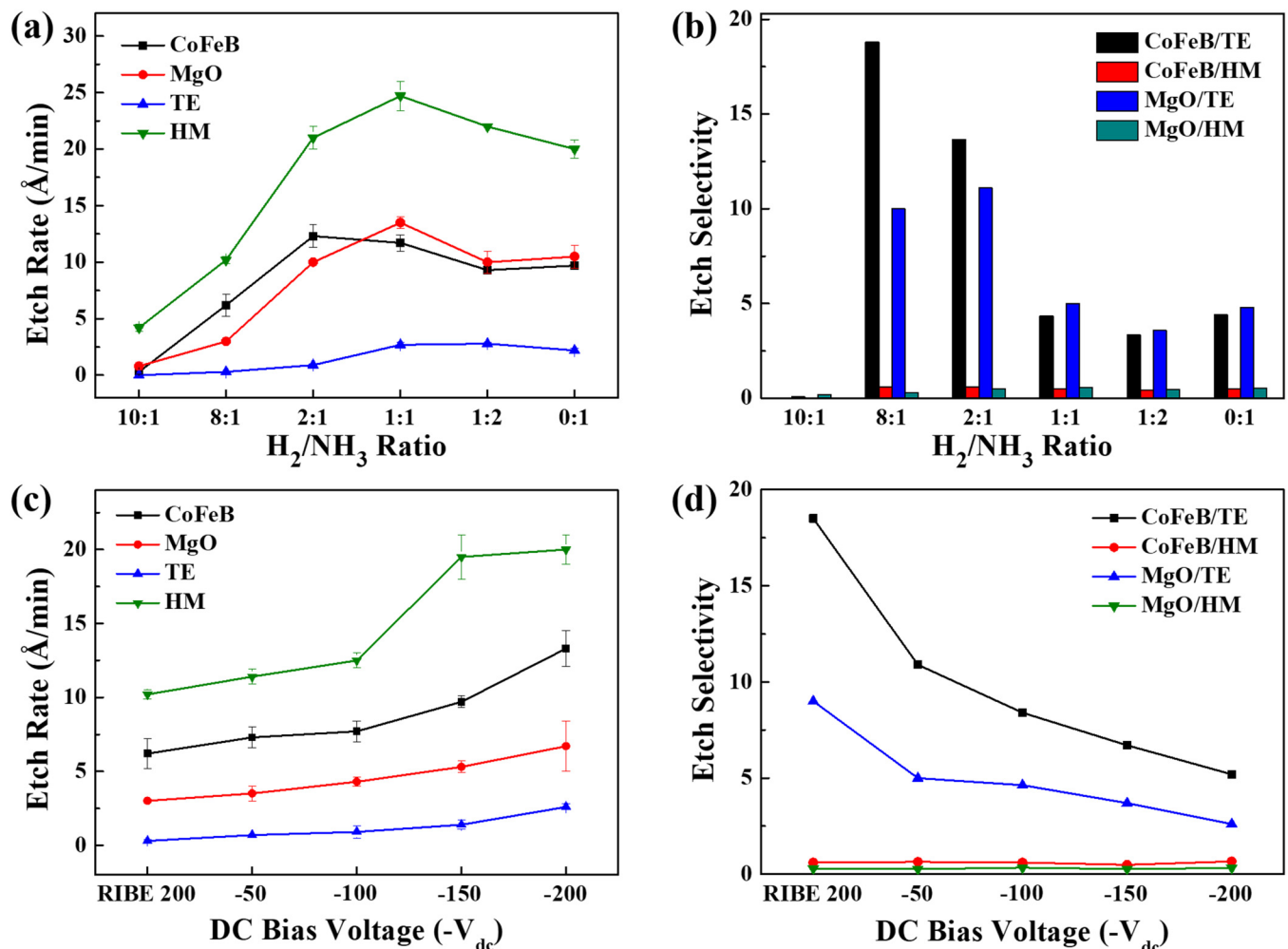

FIG. 2. Etch rates of MTJ materials and hardmask materials and etch selectivities of MTJ materials over the top electrode (TE) and hardmask (HM). (a) Etch rates and (b) etch selectivities measured as a function of H_2/NH_3 ratio during RIBE. (c) Etch rates and (d) etch selectivities measured as a function of V_{dc} for rf-biased RIBE.

pressure, +200 V of first grid voltage, and −250 V of second grid voltage were used while applying 300 W to the ion beam ICP source. As shown in Fig. 2(a), the decreased ratio of H_2/NH_3 initially increased the etch rates of MTJ and mask materials; however, when the ratio of H_2/NH_3 is sufficiently low (≤2:1), the etch rates of MTJ materials and HM were decreased with the decrease in the H_2/NH_3 ratio, and their etch rates were the highest at the H_2/NH_3 ratios between 2:1 and 1:2 while the etch rate of TE was nearly saturated at the H_2/NH_3 ratios lower than 1:1. Figure 2(b) shows the etch selectivities of CoFeB/mask materials, and as shown in Fig. 2(b), the etch selectivity of CoFeB/TE was generally decreased with the decrease in H_2/NH_3 ratio from ~20 at 8:1 to ~4 at 0:1 while etch selectivities of CoFeB/HM were generally lower than 1 for all of the H_2/NH_3 ratios. At the H_2/NH_3 ratio of ≥10:1, due to the very low etch rate of CoFeB, it was difficult to measure the etch selectivity of CoFeB/TE. The highest etch rates observed at the ratios between 2:1 and 1:1 for MTJ materials and HM are believed to be related to the synergy effect of H and NH_x in the formation of hydrides as described in the previous investigation.[22]

In Fig. 1(b), the ions extracted from the first grid are accelerated by voltage differences between the first grid voltage and second grid voltage and decelerated to the third grid having the ground potential; therefore, the ions emitted from the grid assembly have the energy close to the first grid voltage at the substrate when the substrate holder has the ground potential. However, when the substrate is rf-biased by applying rf power to the substrate holder after the removal of grounding, a negative dc voltage ($-V_{dc}$) is developed on the substrate surface and ions emitted from the grid assembly will be accelerated further to the substrate by the dc bias voltage formed on the substrate holder. For the H_2/NH_3 ratio of 8:1, rf-bias power was applied to the substrate holder (after the removal of grounding connected to the substrate holder) while keeping the first grid voltage of the ICP ion beam source at +200 V. Figures 2(c) and 2(d) show the etch rates of MTJ/mask materials and their etch selectivities, respectively. The addition of $-V_{dc}$ voltage from −50 to −200 V by rf-biasing increased the etch rates of all materials while decreasing the etch selectivities of CoFeB/TE and MgO/TE. The addition of the $-V_{dc}$ voltage by rf-biasing increases the total ion energy of the reactive ions bombarding the substrate by having an electrical potential difference of V = first grid voltage + ($-V_{dc}$). The increased ion bombardment energy to the substrate will increase the etch rates of all materials but will also decrease the etch selectivity by increasing the physical etching effect.

Therefore, the physical etching effect during rf-biasing could be similarly maintained by making first grid voltage V_1 = second grid voltage $V_2 + V_{dc}$. Figures 3(a) and 3(b) show the etch rates of MTJ and mask materials and their etch selectivities, respectively, measured for different $-V_{dc}$ to the substrate while maintaining the same electrical potential differences of ~250 V by varying the first grid voltage together with $-V_{dc}$. As shown in Fig. 3(a), the increase in $-V_{dc}$ while keeping the electrical potential similar to ~250 V by decreasing the first grid voltage decreased the etch rates slowly possibly due to the decreased ion flux extracted from the ion beam source at the lower first grid voltage (due to decreased voltage differences between first grid voltage and second grid voltage maintained at −250 V). However, as shown in
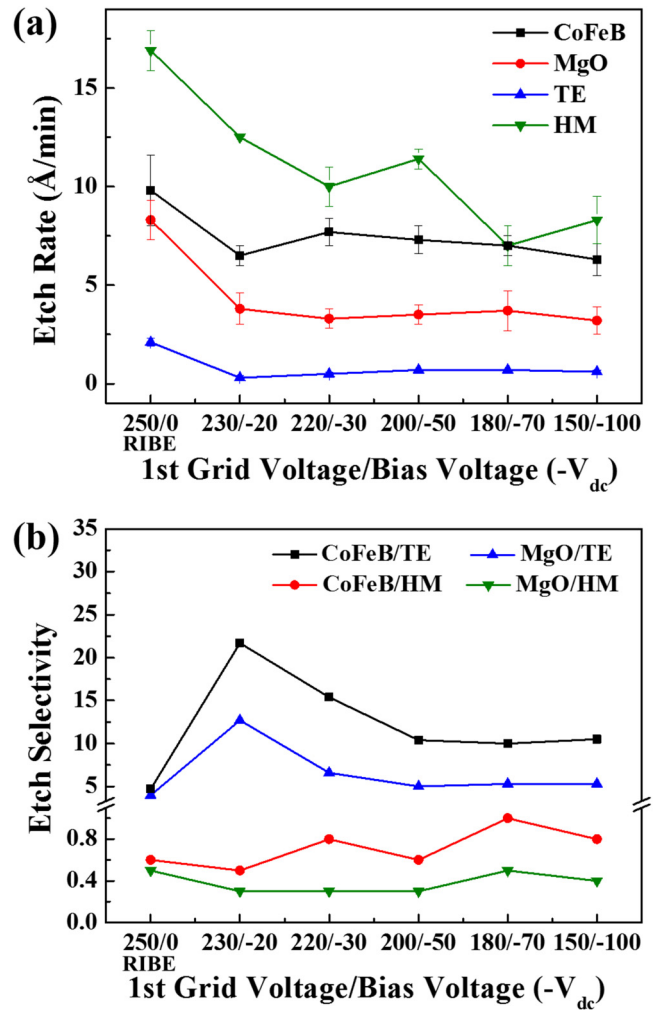

(a)

(b)

FIG. 3. (a) Etch rates of MTJ and hard mask materials and (b) etch selectivities of MTJ materials over mask materials of TE and HM according to different first grid V/$-V_{dc}$ ratios while maintaining the total electrical potential fixed at ~250 V.

Fig. 3(b), when a low $-V_{dc}$ of approximately −20 V was applied to the substrate, the etch selectivities of CoFeB/TE and MgO/TE were increased significantly from ~4.6 and ~4 (for 250/0 of RIBE, that is, at grounded substrate) to 22 and 13 (for 250/−20 V of rf-biased RIBE), respectively, even though the further increase in $-V_{dc}$ to −100 V decreased the etch selectivity. For etch selectivities of MTJ/HM, the etch selectivities were generally lower than 1, and no significant changes in the etch selectivity with $-V_{dc}$ were observed.

Figure 4(a) shows the surface composition of CoFeB and TE (composed of AB) measured by XPS before and after etching using RIBE and rf-biased RIBE with the conditions of 250/0 and 230/−20 (first grid voltage/$-V_{dc}$), respectively, and 8:1 ratio of H_2/NH_3 in Fig. 3. During etching with 8:1 of H_2/NH_3 ratio, due to the
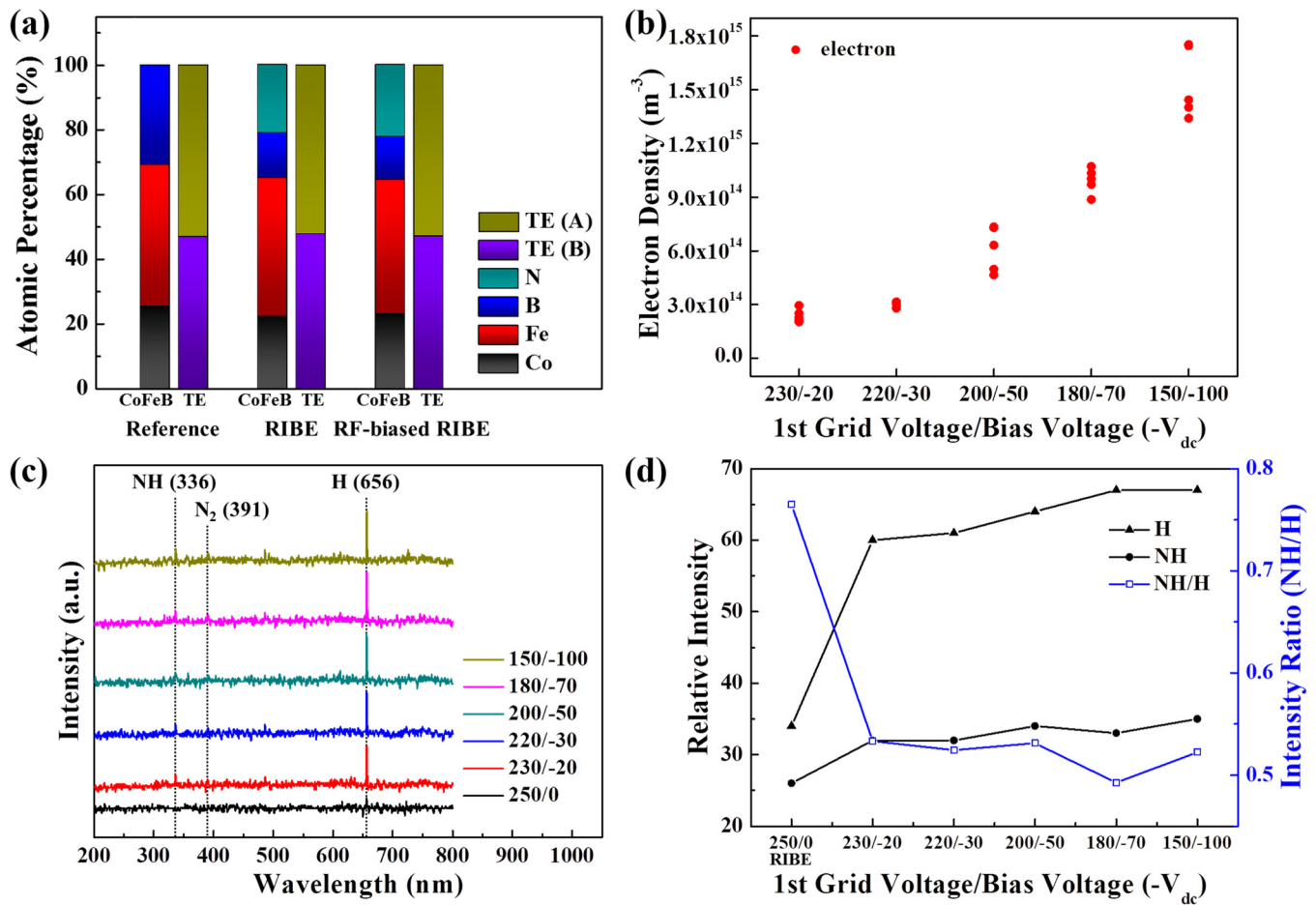
FIG. 4. (a) Surface compositions measured by XPS, (b) electron density measured by a Langmuir probe, (c) OES spectra, and (d) optical emission intensities of H and NH, and the ratio of NH/H measured before and after etching by RIBE and rf-biased RIBE. For RIBE, 250/0 was used and the substrate was connected to ground potential, and for rf-biased RIBE, 230/$-$20 was used by applying rf power to the substrate. Other conditions are the same as those in Fig. 3.

nitrogen in the gas mixture, nitrogen was observed on the surface of CoFeB for both RIBE and rf-biased RIBE, but no significant differences in the surface composition between RIBE and rf-biased RIBE could be observed. In the case of TE, the surface composition was similar before and after etching for both RIBE and rf-biased RIBE. The change in plasma density during rf-biased RIBE was observed using a Langmuir probe, and as shown in Fig. 4(b), even though the plasma density is very low in the range of 10^8–10^9/cm^3 due to the low rf power of 35–60 W, the plasma density was slowly increased with increasing $-V_{dc}$. Figure 4(c) shows the optical emission spectra for RIBE and different rf-biased RIBE conditions in Fig. 3, and peak intensities of NH (336 nm), N$_2$ (391 nm), and H (656 nm) could be observed. The change in optical emission intensities of NH and H and the ratio of H/NH as a function of $-V_{dc}$ in Fig. 3 are shown in Fig. 4(d), and as shown in Fig. 4(d), rapid increases in radical intensities of H and NH and a sudden decrease in the NH/H ratio were observed by the application of rf-biasing of

230/$-$20 indicating more H in the plasmas by the application of small rf-biasing. Therefore, even though no differences in the surface chemistry on etched materials were observed due to increases in radicals and the H/NH ratio through the increase in plasma density and high etch selectivities of MTJ/TE appear to be obtained by the application of a small rf-biasing (from 250/0 to 230/$-$20). In Fig. 3, the further increase in $-V_{dc}$ ($-V_{dc} \geq -30$ V) while keeping the same electrical potential of ~250 V not only decreased the etch rates of MTJ materials but also decreased the etch selectivity of MTJ/TE. It is believed that the lower etch rates are related to the lower ion flux from the ion beam source by using the lower first grid voltage for higher $-V_{dc}$. Also, the lower etch selectivity with increasing $-V_{dc}$ at the same electrical potential of first grid V/$-V_{dc}$ might be related to the increased high energy ion flux to the substrate for higher $-V_{dc}$ [the increase in $-V_{dc}$ by increasing rf-bias power increases not only increase the average ion energy (related to $-V_{dc}$) but also increases the ion energy

distribution to the substrate; therefore, higher energy ions to the substrate can be obtained with increasing $-V_{dc}$ at the same first grid $V/-V_{dc}$ and which increases the physical sputter etching effect].

Using the etch conditions of 250/0 of RIBE and 230/−20 of rf-biased RIBE and with 8:1 ratio of H_2/NH_3, the MTJ layers composed of CoFeB and MgO deposited on BE/Si and patterned with a circular dot-shaped mask consisted of HM/TE were etched, and the etch profiles observed by SEM are shown in Fig. 5. Figures 5(a)–5(c) are the cross-sectional views and Figs. 5(d)–5(f) are the top views of the MTJ patterned with the patterned HM/TE before etching of the MTJ layer (reference), after the etching by RIBE, and after etching by rf-biased RIBE, respectively. For etching by RIBE, the substrate holder was grounded, and for etching by rf-biased RIBE, the substrate holder was connected to 12.56 MHz rf power through a matching network. To etch the MTJ layer, the samples were exposed to RIBE for ~23 min and to rf-biased RIBE for

~28 min. As shown in Figs. 5(a)–5(c), the mask thickness of HM/TE was decreased after the etching MTJ layer with RIBE and rf-biased RIBE, respectively. Even though the etch rate was lower for rf-biased RIBE than RIBE, the etch selectivity of the MTJ/mask layer was higher for rf-biased RIBE as observed in Fig. 3. Also, the sidewall angle appears to be more anisotropic for the rf-biased RIBE. The sidewall roughness of the etched MTJ dot-structure was measured to be ~9.7 nm for RIBE while it was ~9.1 nm for rf-biased RIBE (the sidewall roughness of the reference mask was ~8.3 nm). The thicker diameter and the rougher sidewall of the MTJ etched by RIBE compared to that etched by rf-biased RIBE indicate a thicker sidewall residue redeposited during MTJ etching. Therefore, not only more anisotropic etch profiles but also lower sidewall residue were observed for rf-biased RIBE compared to RIBE. The sidewall residues remaining after etching of the MTJ layer using RIBE and rf-biased RIBE were further observed by cross-sectional TEM, and the results are shown in Fig. 6(a) for
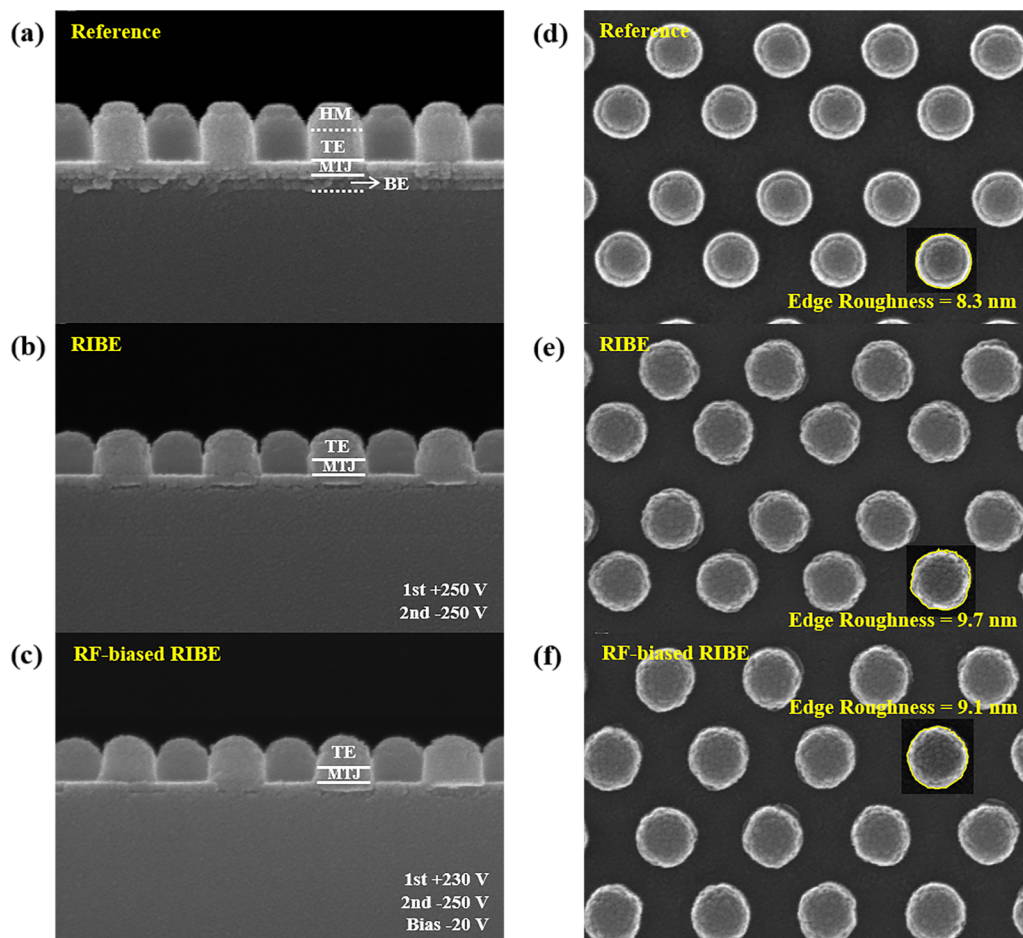
FIG. 5. SEM images before and after etching of the MTJ layer masked with HM/TE dot patterns by RIBE and rf-biased RIBE using H_2/NH_3 for the conditions in Fig. 4. (a)–(c) are the cross-sectional SEM images and (d)–(f) are the top view SEM images before and after etching by RIBE (250/0) and rf-biased RIBE (230/−20), respectively.
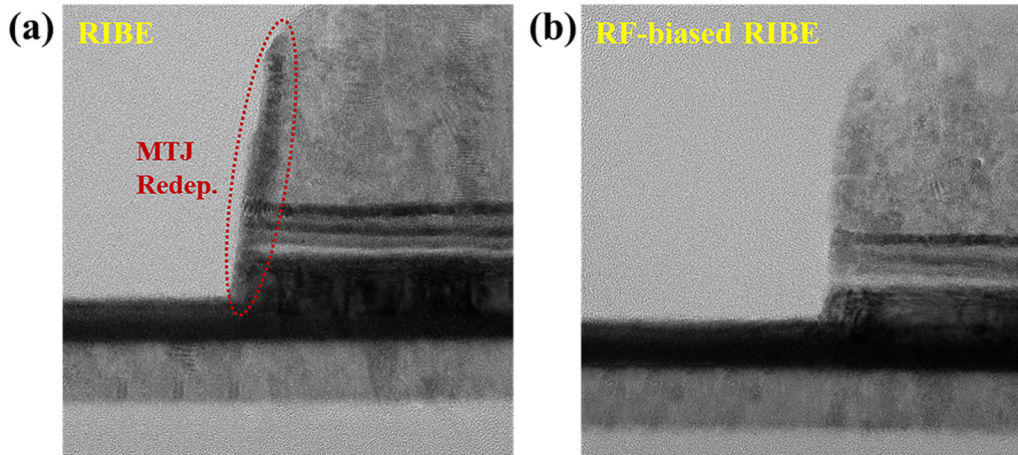
FIG. 6. Cross-sectional TEM images after etching of the MTJ layer masked with HM/TE dot patterns by (a) RIBE (250/0) and (b) rf-biased RIBE (230/−20) using H_2/NH_3 for the conditions in Fig. 4.

RIBE and Fig. 6(b) for rf-biased RIBE. As shown in Fig. 6, a thicker residue and a less anisotropic etch profile were observed on the sidewall of TE and MTJ for RIBE compared to rf-biased RIBE.

In fact, during etching using ion beam, the substrate holder is generally covered with an insulator for electrostatic chucking of the substrate, etc., and to prevent the charging of the substrate, a neutralizer-emitting electron is generally used for IBE, and in the case of RIBE, the neutralizer can be easily damaged by the reactive gas. The CoFeB and MgO were etched again on the metallic substrate covered with a 2 mm thick alumina ceramic for RIBE and rf-biased RIBE, and the results are shown in Fig. 7. As comparison, the etch rates of CoFeB and MgO etched on the metallic substrate holder in Fig. 3(a) are also included. As shown in Fig. 7, when the CoFeB and MgO are located on the ceramic substrate holder without a neutralizer due to the charging of the substrate, the etch rates of CoFeB and MgO were very low for RIBE conditions of 250/0 (for the condition of RIBE condition of 200/0, the etch rates were nearly 0). However, for rf-biased conditions of 230/−20–150/ −100, the etch rates of CoFeB and MgO were similar to those located on the ground metallic substrate holder possibly due to the removal of charging on the substrate by the electrons in the plasma generated above the substrate through rf-biasing during RIBE.

Figure 8 shows charging issues that can occur in RIBE and how to discharge the charged substrate using a neutralizer or rf-biasing as cartoons. Figure 8(a) shows the charging phenomenon that occurs when the substrate is exposed to an ion beam. When insulating substrate (conducting substrate on electrostatic chuck, substrate containing insulating layers, etc.) is etched using IBE, the substrate surface is gradually charged (+) by positive ions. If the substrate surface is sufficiently charged, etching will be stopped by deflecting positive ions reaching the substrate as shown in Fig. 8(a). To solve the charging effect, a neutralizer, an electron emitter made of a heated tungsten filament, is generally used in the IBE as shown in Fig. 8(b), and electrons are supplied to the substrate during etching by emitting electrons through the filament around the

substrate. No filament damage or contamination is observed during etching for Ar^+ ion beam. However, when a neutralizer is used with reactive ion beam using various reactive gases, reactive radicals can react with the neutralizer and generate unwanted contamination and filament damage. Figure 8(c) shows the process of removing charging on the insulating substrate using rf-bias during RIBE without using a neutralizer. During etching using RIBE, by forming an additional low density plasma from rf-biasing, the removal of substrate charging on the insulator substrate during
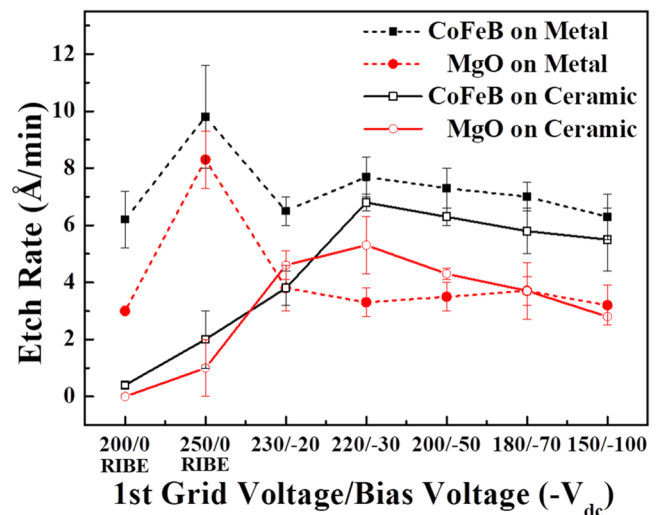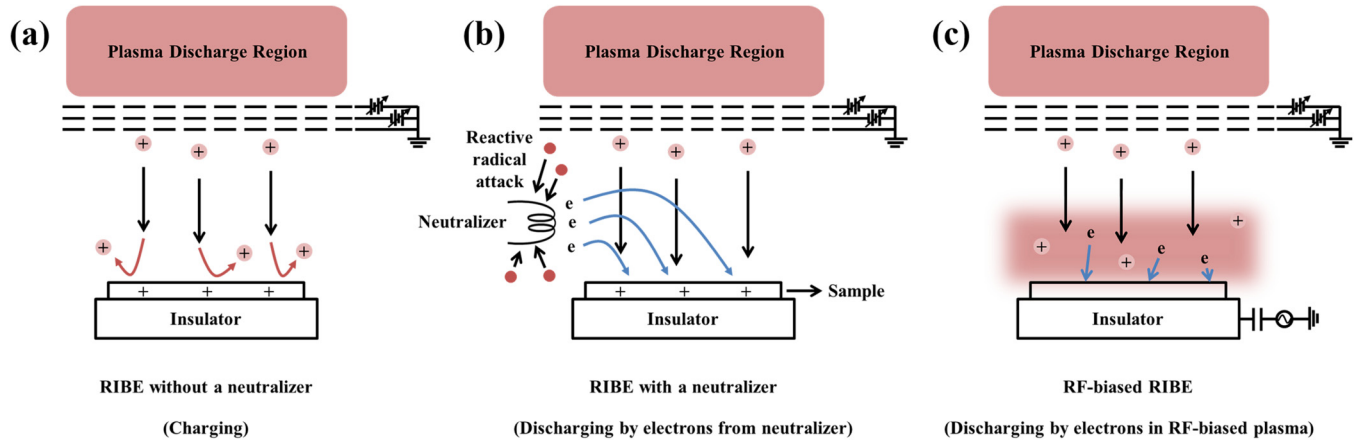

FIG. 7. Comparison of the etch rates of CoFeB and MgO with H_2/NH_3 RIBE and rf-biased RIBE for the etch conditions in Fig. 4 depending on the presence or absence of the ceramic on the metallic substrate holder to evaluate the charging effect.

FIG. 8. Cartoons showing (a) the charging of the substrate on an insulator substrate holder during the RIBE without a neutralizer, (b) the removal of substrate charging on the insulator substrate holder during RIBE by using a neutralizer emitting electrons, and (c) the removal of substrate charging on the insulator substrate holder during RIBE by electrons in the plasma generated by rf-biasing.

RIBE can be achieved by the electrons in the plasma generated by rf-biasing for rf-biased RIBE. (If electronegative gases such as gases containing Cl, F, and Br are used in etching instead of H_2 and NH_3, an additional etching effect by negative ion attachment could be possible during neutralization by negative charges in the plasma.[26,27])

IV. CONCLUSIONS

To improve etch characteristics of the MTJ layer of the MRAM using RIBE, rf power was applied to the substrate during RIBE processing, and the effects of rf-biasing on the etch characteristics of the MTJ material consisting of CoFeB and MgO such as etch rates, etch selectivities over mask materials such as hardmask (HM) and top electrode (TE), and etch profiles masked with dot-patterned HM/TE were investigated using H_2/NH_3 gas mixtures. When rf-biasing was added to a RIBE condition while maintaining the ion bombardment energy to the substrate similarly by decreasing the first grid voltage from the ion beam while increasing $-V_{dc}$ to the substrate by rf-biasing (electrical potential ~first grid $V + V_{dc}$), the highest etch selectivity of MTJ over TE was obtained when a small $-V_{dc}$ of approximately -20 V was added to RIBE. In addition, the improvement in etch anisotropy and thinner sidewall residue on the etched MTJ could be observed. It is believed that the improvement in etch selectivity, the higher etch anisotropy, and thinner sidewall reside on the etched MTJ for the rf-biased RIBE condition with a small $-V_{dc}$ of approximately -20 V are related to the increased H_2/NH_3 gas dissociation and the increased H/NH ratio above the substrate during RIBE. In addition, for etching of MTJ materials located on an insulator substrate holder, a neutralizer (electron emitter) that is generally used to remove charging of the substrate during the IBE was not required for rf-biased RIBE due to the supply of electron for removing the charging of the substrate during RIBE from electrons in the plasma generated by rf-biasing.

AUTHOR DECLARATIONS
Conflict of Interest

The authors have no conflicts to disclose.

Author Contributions

Y.E.K. and D.S.K. contributed equally to this work.

Ye Eun Kim: Conceptualization (equal); Investigation (lead); Writing – original draft (equal). **Doo San Kim:** Conceptualization (equal); Methodology (lead); Writing – original draft (equal). **Yun Jong Jang:** Data curation (supporting). **Hong Seong Gil:** Data curation (supporting). **Ho Seop Jeon:** Formal analysis (supporting). **Jong Woo Hong:** Formal analysis (supporting). **In Ho Kim:** Funding acquisition (equal). **Cheol Kim:** Funding acquisition (equal). **Jeong-Heon Park:** Funding acquisition (equal). **Geun Young Yeom:** Supervision (lead); Writing – review & editing (lead).

DATA AVAILABILITY

The data that support the findings of this study are available from the corresponding author upon reasonable request.

REFERENCES

[1]R. L. Comstock, J. Mater. Sci.: Mater. Electron. **13**, 509 (2002).
[2]T. Kishi *et al.*, *IEEE International Electron Devices Meeting*, San Francisco, CA, 15–17 December 2008 (IEEE, New York, 2008), p. 1.
[3]A. D. Kent and D. C. Worledge, Nat. Nanotechnol. **10**, 187 (2015).
[4]S. Ikeda *et al.*, Nat. Mater. **9**, 721 (2010).
[5]H. Kubota *et al.*, Jpn. J. Appl. Phys. **44**, L1237 (2005).

[6]J. C. Slonczewski, J. Magn. Magn. Mater. **159**, L1 (1996).

[7]S. Kumagai, T. Shiraiwa, and S. Samukawa, J. Vac. Sci. Technol. A **22**, 1093 (2004).

[8]H.-W. Ra, Y. B. Hahn, K. S. Song, M. H. Park, and Y. K. Hong, J. Vac. Sci. Technol. A **22**, 2388 (2004).

[9]H. Gokan and S. Esho, J. Vac. Sci. Technol. **18**, 23 (1981).

[10]K. Sugiura et al., Jpn. J. Appl. Phys. **48**, 08HD02 (2009).

[11]J. Jeong and T. Endoh, Jpn. J. Appl. Phys. **56**, 04CE09 (2017).

[12]M. H. Ji et al., AIP Adv. **9**, 085317 (2019).

[13]W. Zhao et al., Materials **9**, 41 (2016).

[14]V. D. Nguyen et al., IEEE International Electron Devices Meeting, San Francisco, CA, 2–6 December 2017 (IEEE, New York, 2017), pp. 38.5.1–38.5.4.

[15]Y. Otani, H. Kubota, A. Fukushima, H. Maehara, T. Osada, S. Yuasa, and K. Ando, IEEE Trans. Magn. **43**, 2776 (2007).

[16]D. S. Kim, J. E. Kim, Y. J. Gill, Y. J. Jang, Y. E. Kim, K. N. Kim, G. Y. Yeom, and D. W. Kim, Appl. Sci. Converg. Technol. **29**, 41 (2020).

[17]E. H. Kim, T. Y. Lee, and C. W. Chung, J. Electrochem. Soc. **159**, H230 (2012).

[18]J. Y. Park, S. K. Kang, M. H. Jeon, M. S. Jhon, and G. Y. Yeom, J. Electrochem. Soc. **158**, H1 (2011).

[19]M. H. Jeon, K. C. Yang, J. W. Park, D. H. Yun, K. N. Kim, and G. Y. Yeom, J. Vac. Sci. Technol. B **33**, 061212 (2015).

[20]M. H. Jeon, K. C. Yang, J. W. Park, D. H. Yun, K. N. Kim, and G. Y. Yeom, J. Nanosci. Nanotechnol. **16**, 11823 (2016).

[21]K. Kinoshita, T. Yamamoto, H. Honjo, N. Kasai, S. Ikeda, and H. Ohno, Jpn. J. Appl. Phys. **51**, 08HA01 (2012).

[22]J. E. Kim et al., Nanotechnology **32**, 055301 (2021).

[23]D. S. Kim et al., Appl. Surf. Sci. **571**, 151311 (2022).

[24]X. Wang, Y. Liu, X. Xu, S. Fu, and Z. Cui, J. Vac. Sci. Technol. A **24**, 1067 (2006).

[25]G. Y. Yeom, U.S. patent 17/752,199 (24 November 2022).

[26]H. Ohtake, S. Samukawa, H. Oikawa, and Y. Nashimoto, Jpn. J. Appl. Phys. **37**, 2311 (1998).

[27]T. Mukai, N. Ohshima, H. Hada, and S. Samukawa, J. Vac. Sci. Technol. A **25**, 432 (2007).